

# MicroRNA expression profile is altered in the upper airway skeletal muscle tissue of patients with obstructive sleep apnea-hypopnea syndrome

Journal of International Medical Research

2019, Vol. 47(9) 4163–4182

© The Author(s) 2019

Article reuse guidelines:

[sagepub.com/journals-permissions](http://sagepub.com/journals-permissions)

DOI: 10.1177/0300060519858900

[journals.sagepub.com/home/imr](http://journals.sagepub.com/home/imr)



Jin Hou<sup>1</sup>, Lei Zhao<sup>2</sup>, Jing Yan<sup>1</sup>, Xiaoyong Ren<sup>1</sup>,  
Kang Zhu<sup>1</sup>, Tianxi Gao<sup>1</sup>, Xiaoying Du<sup>1</sup>,  
Huanan Luo<sup>1</sup>, Zhihui Li<sup>1</sup> and Min Xu<sup>1</sup> 

## Abstract

**Objective:** To investigate the involvement of microRNAs (miRNAs) in the pathogenesis of obstructive sleep apnea-hypopnea syndrome (OSAHS).

**Methods:** In this study, we investigated miRNA profiles in the upper airway (UA) skeletal muscles of four patients with OSAHS and four matched controls using the miRCURY miRNA array. In another cohort of 12 OSAHS cases and 7 controls, the mRNA expression levels of interleukin (IL)-6 and Lin-28 homolog A (Lin28A), targets of the downregulated let-7 family members, were measured by real-time quantitative-PCR. The potential targets of the miRNAs were predicted by miRNA target prediction databases miRanda, Microcosm, and Targetscan.

**Results:** The array identified 370 differentially expressed miRNAs, of which 181 were upregulated and 189 were downregulated in OSAHS patients (based on a fold-change >2.0 and  $p < 0.05$ ). Upregulation of IL-6 and Lin28A was validated by quantitative reverse transcription PCR. The 612 targets predicted by all three algorithms were subjected to gene ontology (GO) and Kyoto Encyclopedia of Genes and Genomes (KEGG) pathway analyses. The results revealed perturbations in signaling pathways and cellular functions.

<sup>1</sup>Department of Otorhinolaryngology, the Second Affiliated Hospital, Medical School of Xi'an Jiaotong University, Xi'an, China

<sup>2</sup>Department of Molecular Physiology and Biophysics, University of Iowa Carver College of Medicine, Iowa City, IA, USA

## Corresponding author:

Min Xu, Department of Otorhinolaryngology, the Second Affiliated Hospital, Medical School of Xi'an Jiaotong University, 157 Xiwu Road, Xi'an 710004, Shaanxi, China.  
Email: 13319251982@126.com



**Conclusion:** This study demonstrated profoundly altered miRNA expression profiles in upper airway muscular tissues of patients with OSAHS, which might contribute to the formation and development of OSAHS.

### Keywords

Obstructive sleep apnea-hypopnea syndrome, OSAHS, upper airway muscle, microRNA, microarray, IL-6, Lin28A

Date received: 17 December 2018; accepted: 31 May 2019

## Introduction

Obstructive sleep apnea-hypopnea syndrome (OSAHS) is a common chronic disease characterized by repetitive episodes of upper airway (UA) collapse during sleep.<sup>1</sup> These episodes are associated with brain arousals that disturb the patient's sleep and therefore lead to excessive daytime sleepiness and fatigue.<sup>1</sup> The prevalence of OSAHS is 5% to 14% among adults aged 30 to 70 years and up to 45% in the obese population.<sup>2</sup> The repetitive episodes of hypoxia can result in a series of pathophysiologic consequences, including metabolic disturbances,<sup>3,4</sup> systemic inflammation,<sup>5</sup> and cardiovascular diseases.<sup>6</sup> Therefore, OSAHS represents a major public health concern, and understanding its pathogenesis is essential in the prevention and treatment of this disease.

OSAHS is a multifactorial disease. The most important pathophysiological factors of OSAHS include UA collapsibility, anatomical abnormalities, and pharyngeal muscular dysfunction.<sup>7,8</sup> In addition to these anatomical factors, involvement of systemic and local inflammation in the development of OSAHS have been reported.<sup>9,10</sup> Intermittent hypoxia caused by OSAHS has been associated with systematic inflammation with production of inflammatory cytokines such as

interleukin-6 (IL-6) and tumor necrosis factor-alpha (TNF- $\alpha$ ).<sup>11-13</sup> However, it is still unclear whether systemic inflammation is the cause or the result of OSAHS. Moreover, repeated snoring, hypoxia, and other factors may lead to mechanical trauma and local inflammation of UA muscle tissues.<sup>14</sup> These factors may lead, in turn, to alterations in muscle fiber structure, which forms the histological basis for the dysfunction of UA or lower pharynx neuromuscular tissues during sleep. Furthermore, a variety of other factors have been identified in the pathogenesis of OSAHS, such as obesity,<sup>15</sup> generation of reactive oxygen species (ROS) due to oxidative imbalance,<sup>16</sup> genetic factors,<sup>17</sup> and altered matrix metalloproteinase expression in the palatopharyngeal muscles.<sup>18</sup> Despite the rapidly growing body of studies in OSAHS, its exact etiopathogenesis remains largely unknown.

MicroRNAs (miRNAs) are small (22 to 25 nt) noncoding RNA molecules that negatively regulate gene expression primarily by binding to the 3' untranslated regions (3' UTR) of mRNA transcripts to repress their translation or promote their degradation.<sup>19</sup> Even subtle changes in miRNA expression may lead to significant alterations in cellular function. Therefore, miRNAs have emerged as key regulators of diverse biological processes, including

development, differentiation, cell apoptosis, and proliferation.<sup>20</sup> Recent studies have revealed that miRNAs are associated with OSAHS-related morbidities. Gharib et al.<sup>21</sup> reported that sleep fragmentation, a major consequence of OSAHS, caused dysregulated expression of miRNAs (19 differentially expressed miRNAs were identified) and profound transcriptional perturbations, which were associated with interruption of signaling pathways particularly involved in metabolic regulation, in mouse visceral adipocytes. An et al.<sup>22</sup> showed that miR-130a was involved in the progression of OSAHS-associated pulmonary hypertension by downregulating the growth arrest-specific homeobox (GAX) gene. However, the involvement of miRNAs in the pathogenesis of OSAHS itself has not been reported.

Altered expression of miRNAs has been reported to occur on exposure to hypoxia,<sup>23</sup> mechanical stimulation,<sup>24</sup> and inflammation,<sup>25</sup> among other factors. The altered miRNA expression profile in turn may affect these processes. Therefore, we hypothesized that the miRNA expression profile is profoundly altered in the UA tissues of patients with OSAHS. Accordingly, the primary goal of this study was to identify differentially expressed miRNAs in UA muscle tissues of OSAHS patients and to explore the potential role(s) of these miRNA in the development of OSAHS.

## Materials and methods

### *Human subjects and sample collection*

This study was performed with the approval of the Xi'an Jiaotong University ethics committee. All the participants gave informed consent before beginning the study.

This study included 22 patients with OSAHS, aged 25 to 48 years, who were diagnosed between January 1, 2015, and December 31, 2016. Another 17 patients

with chronic tonsillitis were included as the control group. All patients were recruited from the Department of Otolaryngology at the Second Affiliated Hospital of Xi'an Jiaotong University. All patients were monitored by using overnight polysomnography (PSG). All 22 patients had severe OSAHS, defined by an apnea-hypopnea index (AHI) >30 (i.e., the number of apnea events per hour), whereas the individuals with chronic tonsillitis (control group) had no or minimal OSAHS (AHI <5). Age, sex, height, weight, smoking and drinking histories, laboratory data on metabolic variables, and PSG findings were collected from participants' medical records. The demographic and clinical characteristics of the patients and controls are summarized in Table 1, Table 2, and Table 3.

Upper airway skeletal muscle tissue (about  $0.5 \times 0.5 \text{ cm}^2$ ) was collected under surgery from the hypertrophy soft palate tissue of patients with OSAHS and from the area around the tonsils of individuals in the control group. Within 30 minutes of collection, the samples were washed with PBS, snap frozen in liquid nitrogen, and stored in a  $-80^\circ\text{C}$  freezer before extraction of total RNA.

### *RNA extraction*

Total RNA was isolated using TRIzol reagent (Invitrogen Corp., Carlsbad, CA, USA) and further purified with the miRNeasy mini kit (Qiagen, Valencia, CA, USA) according to the manufacturer's instructions. RNA concentration and purity were measured by using the ND-1000 Nanodrop spectrophotometer (Nanodrop Technologies/Thermo Fisher Scientific, Waltham, MA, USA). Samples with a ratio of absorbance at 260 and 280 nm between 1.8 and 2.1 were considered acceptable. Electrophoresis was used to analyze RNA integrity, and only samples

**Table 1.** Baseline characteristics of patients with OSAHS and controls.

	OSAHS group (n=22)	Control group (n=17)	p-value
Age (years)	34.86 ± 1.43	35.24 ± 2.12	0.881
Male [no. (%)]	17 (77)	12 (65)	0.400
BMI (kg/m <sup>2</sup> )	29.64 ± 0.95	26.13 ± 0.81	0.620
TG (mmol/L)	2.97 ± 0.47	1.27 ± 0.26	0.006**
Fasting blood glucose (mmol/L)	5.18 ± 0.24	4.54 ± 0.18	0.051
AHI (events/hour)	69.20 ± 4.12	1.99 ± 0.24	0.001**
Minimum oxygen saturation (%)	59.73 ± 2.41	92.12 ± 0.47	0.001**
Average oxygen saturation (%)	88.39 ± 1.00	97.28 ± 0.27	0.001**
WBC (× 10 <sup>6</sup> /L)	7.28 ± 0.28	6.36 ± 0.45	0.078
Smoking history [no. (%)]	5 (22.7)	4 (23.5)	0.521
Drinking history [no. (%)]	8 (36.4)	6 (35.2)	483

OSAHS = obstructive sleep apnea-hypopnea syndrome, BMI = body mass index, TG = triglyceride, AHI = apnea-hypopnea index, WBC = white blood cell. Data represent the mean ± standard error (SEM) or percentage of each group.

\*\*p < 0.01: difference between the two groups by Mann-Whitney test or chi-squared test.

**Table 2.** Baseline characteristics of OSAHS patients and controls in qRT-PCR validation of the microarray results.

	OSAHS group (n=10)	Control group (n=10)	p-value
Age (years)	35.21 ± 1.86	36.83 ± 1.97	0.362
Male [no. (%)]	7 (70.0)	5 (50.0)	0.055
BMI (kg/m <sup>2</sup> )	30.14 ± 1.05	27.56 ± 1.33	0.063
TG (mmol/L)	3.25 ± 0.63	1.59 ± 0.22	0.008**
Fasting blood glucose (mmol/L)	5.39 ± 0.32	4.93 ± 0.26	0.062
AHI (events/hour)	72.35 ± 5.06	2.03 ± 1.25	0.001**
Minimum oxygen saturation (%)	50.11 ± 4.67	94.42 ± 0.69	0.001**
Average oxygen saturation (%)	86.75 ± 1.62	97.58 ± 0.56	0.001**
WBC (× 10 <sup>6</sup> /L)	7.85 ± 0.43	7.03 ± 0.73	0.125
Smoking history [no. (%)]	3 (30.0)	2 (20.0)	0.052
Drinking history [no. (%)]	5 (50.0)	4 (40.0)	0.077

OSAHS = obstructive sleep apnea-hypopnea syndrome, BMI = body mass index, TG = triglyceride, AHI = apnea-hypopnea index, WBC = white blood cell. Data represent the mean ± standard error (SEM) or percentage of each group.

\*\*p < 0.01: difference between the two groups by Mann-Whitney test or chi-squared test.

with 28S/18S >2 were accepted in the present study.

### MiRNA labeling and array hybridization

The differentially expressed miRNAs between OSAHS patients and the control group were identified by using the miRCURY LNA microRNA Array (v.18.0, Exiqon, Vedbæk, Denmark). The

microarray analysis was conducted by Kangcheng Bio-science Service Company (Shanghai, China). After passing quality control, miRNAs were labeled using the mercury Hy3/Hy5 Power labeling kit (Exiqon) according to the manufacturer's instructions. Briefly, 1 µg of RNA in 2.0 µl of water was mixed with 1.0 µl of calf intestine phosphatase (CIP) buffer and CIP

**Table 3.** Baseline characteristics of OSAHS patients and controls in qRT-PCR for IL-6 and Lin28A expression levels.

	OSAHS group (n=12)	Control group (n=7)	p-value
Age (years)	33.96 ± 1.61	34.29 ± 1.92	0.903
Male [no. (%)]	10 (45.5)	7 (41.2)	0.821
BMI (kg/m <sup>2</sup> )	28.24 ± 1.13	25.82 ± 0.79	0.315
TG (mmol/L)	2.08 ± 1.28	1.03 ± 0.64	0.009**
Fasting blood glucose (mmol/L)	4.62 ± 0.43	4.27 ± 0.24	0.005
AHI (events/hour)	66.34 ± 5.87	1.20 ± 0.34	0.001**
Minimum oxygen saturation (%)	63.16 ± 3.62	91.02 ± 1.85	0.001**
Average oxygen saturation (%)	90.42 ± 1.21	96.28 ± 0.72	0.001**
WBC (×10 <sup>6</sup> /L)	6.82 ± 0.34	6.21 ± 0.56	0.740
Smoking history [no. (%)]	2 (16.7)	2 (28.6)	0.061
Drinking history [no. (%)]	3 (25.0)	2 (28.6)	0.483

OSAHS = obstructive sleep apnea-hypopnea syndrome, BMI = body mass index, TG = triglyceride, AHI = apnea-hypopnea index, WBC = white blood cell. Data represent the mean ± standard error (SEM) or percentage of each group.

\*\**p* < 0.01: difference between the two groups by Mann-Whitney test or chi-squared test.

enzyme from the labeling kit. The mixture was incubated for 30 minutes at 37°C, and the reaction was terminated by incubation for 5 minutes at 95°C. Then, 3.0 µl of labeling buffer, 1.5 µl of fluorescent label (Hy3), 2.0 µl of dimethyl sulfoxide (DMSO), and 2.0 µl of labeling enzyme were added into the mixture. The labeling reaction was incubated for 1 hour at 16°C and terminated by incubation for 15 minutes at 65°C. After the labeling procedure was stopped, the Hy3-labeled samples were hybridized on the miRCURY LNA microRNA array according to the manufacturer's instructions. Briefly, the total 25 µl mixture from Hy3-labeled samples with 25 µl of hybridization buffer were denatured for 2 minutes at 95°C, incubated on ice for 2 minutes, and then hybridized to the microarray for 16 to 20 hours at 56°C in a 12-Bay Hybridization System (NimbleGen Systems Inc., Madison, WI, USA). Following hybridization, the slides were washed several times with the washing buffer and scanned using the Axon GenePix 4000B microarray scanner (Axon Instruments, Union City, CA, USA).

### Microarray data analysis

Scanned images were then imported into the GenePix Pro 6.0 software (Axon Instruments) for grid alignment and data extraction to obtain the signal intensity of each spot. After normalization, the obtained average value for each miRNA was used for statistics. The raw and normalized array datasets have been deposited in the NCBI Gene Expression Omnibus (GEO) database (<http://www.ncbi.nlm.nih.gov/>) under accession number GSE99239. Differentially expressed miRNAs between the two groups were filtered by two criteria: fold change ≥ 2 (upregulated) or < 0.5 (downregulated) and *p*-value < 0.05. The results are presented as fold changes in miRNA expression. The expression profiles of the differentially expressed miRNAs between the two groups were then subjected to hierarchical clustering.

### Quantitative reverse transcription PCR validation of the microarray results

To validate the initial microarray results, we measured the levels of 10 differentially

expressed miRNAs by quantitative reverse transcription (qRT)-PCR in 10 OSAHS patients and 10 controls (a subset of the 22 patients and 17 controls in the main study). Total RNA was isolated from 50 to 100 mg of tissue homogenates using TRIzol reagent as described above. The quality and quantity of extracted RNA were measured using a NanoDrop ND-1000 spectrophotometer. Target miRNAs were transcribed to cDNA using a cDNA Synthesis kit (Epicentre, Madison, WI, USA) with specific reverse transcription primers (listed in Table S1) according to the manufacturer's instructions. Then, the cDNA was subjected to qRT-PCR by using the Arraystar SYBR Green Real-time qPCR Master Mix (Arraystar, Rockville, MD, USA) with specific primers (listed in Table S2). Each reaction mixture contained 5  $\mu$ l of master mix, 0.5  $\mu$ l of miR-RT primers F (10  $\mu$ M), 0.5  $\mu$ l of miR-RT primers R (10  $\mu$ M), and 2  $\mu$ l of RNase-free H<sub>2</sub>O. Finally, 2  $\mu$ l of the corresponding template cDNA was added to each reaction. The qRT-PCR reactions were performed using the ABI Prism 7900 system (Applied Biosystems, Foster City, CA, USA) under the following conditions: 1 cycle of pre-incubation, 95°C for 10 minutes; 45 cycles of amplification, each consisting of denaturation at 95°C for 10 s, annealing and elongation at 60°C for 60 s; and 1 cycle of melting at 95°C for 10 s, 60°C for 1 minute, heating to 95°C for 15 s; U6 small nuclear (sn)RNA was used as an internal reference. Each sample was analyzed in triplicate. The expression level of each miRNA was normalized to the U6 level and the fold change was calculated using the  $2^{-\Delta\Delta CT}$  method.

#### *qRT-PCR for IL-6 and Lin28A expression levels*

The mRNA expression levels of IL-6 and Lin-28 homolog A (Lin28A) were measured

by qRT-PCR in a second cohort that included 12 OSAHS cases and 7 controls (a subset of the 22 patients and 17 controls in the main study). Total RNA was isolated from 50 to 100 mg of tissue homogenate using TRIzol reagent as described above. For each sample, 0.5  $\mu$ g of total RNA was reverse transcribed into cDNA with the PrimeScript RT Master Mix kit (Takara) according to the manufacturer's instructions. The reaction mixture contained 4  $\mu$ l of 5 $\times$  master mix, 0.5  $\mu$ g of RNA, and H<sub>2</sub>O to a total volume of 20  $\mu$ l, and the reaction was run at 37°C for 60 minutes followed by 85°C for 5 s. Then, the cDNA was subjected to qRT-PCR by using the Power SYBR Green PCR Master Mix kit (Thermo Fisher Scientific) according to the manufacturer's instructions. Each reaction mixture contained 10  $\mu$ l of master mix, 1.0  $\mu$ l of forward primer (10  $\mu$ M), 1.0  $\mu$ l of reverse primer (10  $\mu$ M), and 8  $\mu$ l of cDNA. The qRT-PCR reactions were performed using the ABI ViiA 7 real-time PCR system (Thermo Fisher Scientific) under the following conditions: 1 cycle of pre-incubation, 50°C for 3 minutes; 40 cycles of amplification each consisting of denaturation at 95°C for 3 minutes, annealing at 95°C for 10 s, and elongation at 60°C for 30 s; 1 cycle of melting from 60°C to 95°C for 10 s with an increment at 0.5°C. Each sample was analyzed in triplicate. The expression levels of IL-6 and Lin28A were normalized to the level of GAPDH and fold changes were calculated using the  $2^{-\Delta\Delta CT}$  method.<sup>26</sup> Primer sequences were as follows: GAPDH forward: 5'-AGACAGC CGCATCTTCTTGT-3' and reverse: 5'-CTTGCCGTGGGTAGAGTCAT-3'; IL-6 forward: 5'-GCCACTCACCTCTTCAGA ACGA-3' and reverse: 5'-GCCTCTTTGC TGCTTTACAC-3'; Lin28A forward: 5'-CTGGAATCCATCCGTGTCACC-3' and reverse: 5'-ACCTCCACAGTTGTAGCA CCT-3'.

### **Gene ontology and Kyoto Encyclopedia of Genes and Genomes pathway enrichment analyses**

Three miRNA target prediction databases (miRanda, Microcosm, and Targetscan) were used to predict potential target genes of the 6 downregulated miRNAs (hsa-let-7b-5p, hsa-let-7g-5p, hsa-let-7i-5p, hsa-miR-34a-5p, hsa-miR-92a-3p, and hsa-miR-101-3p). The 612 candidate targets predicted by the three algorithms were subjected to gene ontology (GO) and Kyoto Encyclopedia of Genes and Genomes (KEGG) pathway enrichment analyses as described previously.<sup>27,28</sup> A  $p$ -value  $< 0.05$  was considered to indicate significant enrichment.

### **Statistical analysis**

All statistical analyses were performed using the GraphPad Prism 6 software (GraphPad Software Inc., La Jolla, CA, USA). Data are presented as mean  $\pm$  standard error (SEM) or percentage of each group. The differences between two groups were analyzed with the Mann–Whitney test or chi-squared test. A  $p$ -value  $< 0.05$  was considered significant.

## **Results**

### **Clinical characteristics and sleep studies of subjects**

In this study, we recruited 22 OSAHS patients, aged 25 to 48 years, diagnosed with overnight PSG at the Otolaryngology Department of the Second Affiliated Hospital of Xi'an Jiaotong University between 1 January, 2015, and 31 December, 2016. The patients with OSAHS were well matched, in terms of age and sex, with 17 patients with chronic tonsillitis as the control group. All 22 patients had severe OSAHS (AHI  $> 30$ ), and the

17 patients with chronic tonsillitis in the control group had no or minimal OSAHS (AHI  $< 5$ ). In addition, the OSAHS group had obviously decreased minimum oxygen saturation ( $59.73 \pm 2.41\%$  vs.  $92.12 \pm 0.47\%$ ,  $p = 0.001$ ) and average oxygen saturation ( $88.39 \pm 1.00\%$  vs.  $97.28 \pm 0.27\%$ ,  $p = 0.001$ ) compared with the control group. The white blood cell count, as an indicator of systemic inflammation, was in the normal range and did not differ significantly between the two groups, suggesting that repetitive exposure to hypoxia was not associated with occurrence of systemic inflammation in the OSAHS patients. The OSAHS group had significantly higher triglyceride ( $2.97 \pm 0.47$  mmol/L vs.  $1.27 \pm 0.26$  mmol/L,  $p = 0.006$ ) levels compared with the control group. These results suggested that the OSAHS patients had profound abnormality in ventilation status. The fasting blood glucose level and body mass index of the OSAHS patients were numerically higher than those of the controls, although not statistically different. The two groups did not differ significantly in age, sex, or smoking and drinking history. The two subsets of patients used for the array validation and to assess IL-6 and Lin28A expression levels had the same overall clinical characteristics as the main group. The demographic and clinical characteristics of the OSAHS and control groups are summarized in Table 1, Table 2, and Table 3.

### **Differentially expressed miRNAs between the two groups**

To identify differentially expressed miRNAs in UA skeletal muscles, total RNA, including miRNAs of four OSAHS patients and four controls, was subjected to the seventh-generation Exiqon miRCURY LNA miRNAs array assay. This array contains 3100 melting temperature ( $T_m$ )-normalized locked nucleic acid (LNA)-

enhanced capture probes, covering all human miRNAs annotated in miRBase 19.0 and viral miRNAs related to humans. Of the miRNAs assayed, 2076 (67.0%) were detected above the background level. The differentially expressed miRNAs were defined by a fold change  $\geq 2.0$  (up- or downregulated) and  $p < 0.05$ . According to these criteria, 370 miRNAs were differentially expressed, of which 181 were upregulated and 189 downregulated in OSAHS patients compared with controls (Table S4). A volcano plot (Figure 1a) and a heatmap (Figure 1b) of all differentially expressed miRNAs were plotted to better demonstrate the dysregulated miRNAs. The microarray data revealed a global perturbation in the miRNA expression pattern in UA muscle tissues of OSAHS patients.

#### **Validation of differentially expressed miRNAs by qRT-PCR**

To validate the results of miRNA profiling, the Taqman qRT-PCR assay was conducted to measure the expression levels of four upregulated miRNAs (hsa-miR-508-5p, hsa-miR-631, hsa-miR-7-2-3p, and hsa-miR-492) and six downregulated miRNAs (hsa-let-7i-5p, hsa-let-7b-5p, hsa-let-7g-5p, hsa-miR-34a-5p, hsa-miR-92a-3p, and hsa-miR-101-3p) in a cohort of 10 OSAHS patients and 10 controls (Table 4). These miRNAs represented those with high to moderate fold changes on the microarray (Table 2). According to the qRT-PCR results, the expression levels of hsa-miR-508-5p, hsa-miR-631, hsa-miR-7-2-3p, and hsa-miR-492 did not differ significantly between the OSAHS and control groups (all  $p > 0.05$ ), whereas hsa-let-7i-5p, hsa-let-7b-5p, hsa-let-7g-5p, hsa-miR-34a-5p, hsa-miR-92a-3p, and hsa-miR-101-3p were all significantly downregulated in OSAHS patients compared with controls (all at least  $p < 0.01$ ) (Figure 2a-j, Table 4); hsa-miR-101-3p and hsa-miR-92a-3p were the

two most prominently downregulated miRNAs (Figure 2i-j, Table 4).

#### **Prediction of miRNA targets and miRNA-gene regulatory network**

We then identified the predicted target genes of the six downregulated miRNAs (hsa-let-7b-5p, hsa-let-7g-5p, hsa-let-7i-5p, hsa-miR-34a-5p, hsa-miR-92a-3p, and hsa-miR-101-3p) using three computational target predicting databases, miRanda, Microcosm, and Targetscan, which used different algorithms. A total of 11,095 genes were potentially targeted by these six miRNAs, and 612 candidate targets were predicted by all three databases (Figure 3a, Table S4). Only the targets that were predicted by all three algorithms were subjected to further bioinformatics analyses. We then constructed a miRNA-mRNA regulatory network based on the interactions between the six miRNAs and their potential targets to illustrate the key regulatory relationships between them. The network consisted of four distinctly separated groups, which represented four functional groups, and all six miRNAs had a large group of target genes. The three hsa-let-7 family members (hsa-let-7b-5p, hsa-let-7g-5p, and hsa-let-7i-5p), which interacted with relatively more target genes than other miRNAs, represented the most important components in this miRNA-mRNA regulatory network (Figure 3b).

#### **IL-6 and Lin28A mRNA expression was upregulated in OSAHS**

As shown in the network analysis, three let-7 family members (hsa-let-7b-5p, hsa-let-7g-5p, and hsa-let-7i-5p) had a large body of potential targets that are implicated in wide-ranging cellular functions. IL-6, a proinflammatory factor, is reported to be a target of these three miRNAs. Our qRT-PCR data showed that IL-6 was

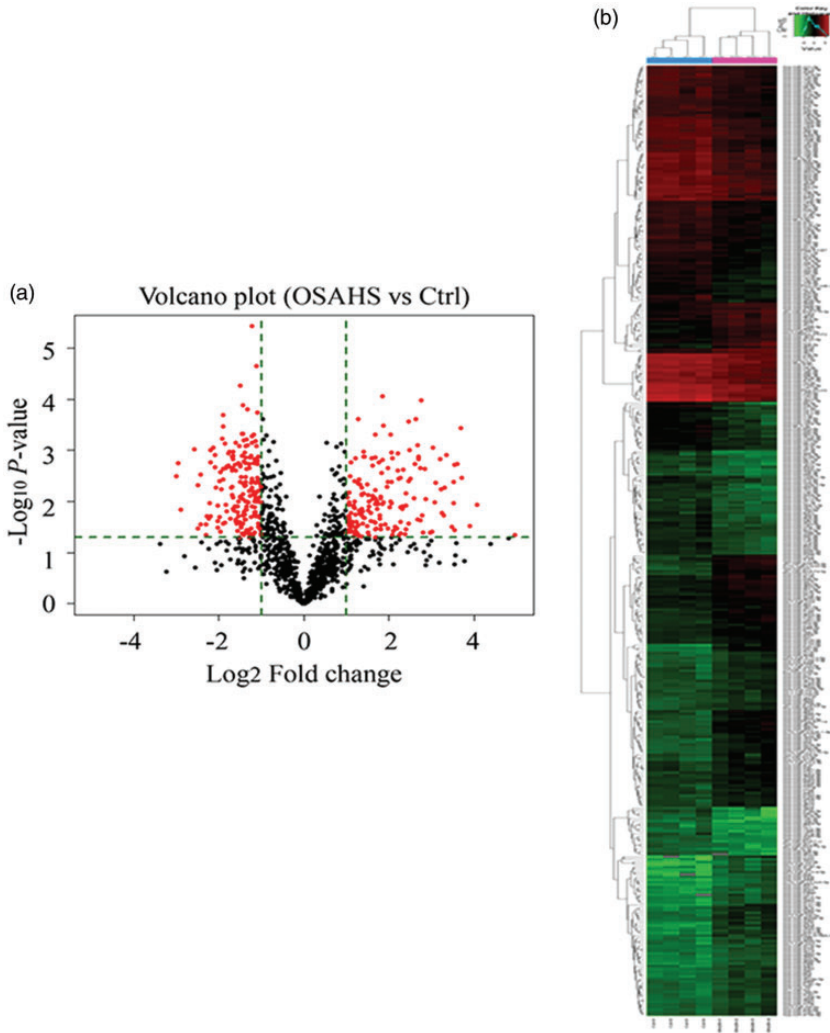


**Figure 1.** Differentially expressed miRNAs between the two groups. Total RNA was isolated from 50 to 100 mg of tissue homogenates of four patients with OSAHS and four controls using TRIzol reagent and subjected to the seventh-generation Exiqon miRCURY LNA miRNA array assay to identify differentially expressed miRNAs. (a) Volcano plot showing the miRNAs identified in the microarray. The red dots represent the differentially expressed miRNAs that met the criteria of fold change  $\geq 2.0$  (up- or downregulated) and  $p < 0.05$ . (b) Unsupervised hierarchical clustering of differentially expressed miRNAs that passed volcano plot filtering. Red: upregulated in OSAHS, green: downregulated in OSAHS. OSAHS, patients with obstructive sleep apnea-hypopnea syndrome; Ctrl, controls (patients with chronic tonsillitis but no OSAHS).

significantly upregulated in the OSAHS group compared with the controls ( $p < 0.05$ , Figure 4a), suggesting that the downregulated let-7 family members might

lead to local inflammation in OSAHS by upregulating IL-6. In this study, Lin28A was upregulated in UA muscle tissues of OSAHS patients ( $p < 0.05$ , Figure 4b),

**Table 4.** qRT-PCR validation of 10 selected differentially expressed miRNAs.

ID	miRNA	Fold change on array (OSAHS vs. control)	Fold change by qRT-PCR (OSAHS vs. control)	p-value (qRT-PCR)
42812	hsa-miR-508-5p	16.806	1.230	0.2179
42700	hsa-miR-631	12.920	1.041	0.7055
42964	hsa-miR-7-2-3p	9.434	0.803	0.1528
42661	hsa-miR-492	2.271	0.908	0.4650
9938	hsa-let-7i-5p	0.471	0.561	0.0008***
168586	hsa-miR-34a-5p	0.467	0.536	0.0017***
147165	hsa-let-7b-5p	0.417	0.548	0.0005***
46438	hsa-let-7g-5p	0.355	0.501	0.0001***
145693	hsa-miR-92a-3p	0.343	0.359	0.0001***
31026	hsa-miR-101-3p	0.285	0.405	0.0001***

\*\*\* $p < 0.01$ , \*\* $p < 0.001$ : means of the OSAHS group and controls were compared by *t*-test.

suggesting that a negative regulatory loop might exist, accounting for the downregulation of the three let-7 miRNAs.

### GO and miRNA-GO network analysis

To gain further insight into the cellular processes potentially mediated by the six down-regulated miRNAs, GO function enrichment analysis was performed to explore the functional roles of their target genes under the domains of biological processes, cellular components, and molecular functions. In terms of biological process, the candidate targets were mainly enriched in “anatomical structure morphogenesis,” “multicellular organismal development,” and “system development” (Figure 5a). The top enriched cellular components were involved in “SWI/SNF superfamily-type complex,” “intracellular part,” and “ESC/E(Z) complex” (Figure 5b). The top enriched molecular functions included “protein binding,” “guanyl-nucleotide exchange factor activity,” and “phosphate metabolic process” (Figure 5c). The complete list of the enriched GO functions is summarized in Table S5. In addition, we constructed a miRNA-GO network to further understand the key biological functions

of the six miRNAs. As shown in Figure 5d, the six miRNAs were mainly associated with cellular metabolic processes, such as macromolecular metabolism and organic substance metabolism.

### KEGG pathway analysis and miRNA-pathway network

KEGG pathway enrichment analysis was performed to identify significant pathways enriched in the target genes of the six miRNAs, with a Fisher *p*-value  $< 0.05$  as the cut-off criterion. The results indicated that 30 KEGG pathways were significantly enriched; the most highly enriched pathways included the MAPK signaling pathway, amyotrophic lateral sclerosis (ALS) pathway, and glycosaminoglycan biosynthesis pathway. The top 10 enriched signaling pathways are illustrated in Figure 6a and the complete list of enriched pathways is provided in Table S6. Next, to further illustrate the key signaling pathways that were potentially regulated by the six miRNAs, we built a miRNA-pathway network (Figure 6b). The six miRNAs were mainly involved in regulating the MAPK pathway, the cAMP pathway, and the

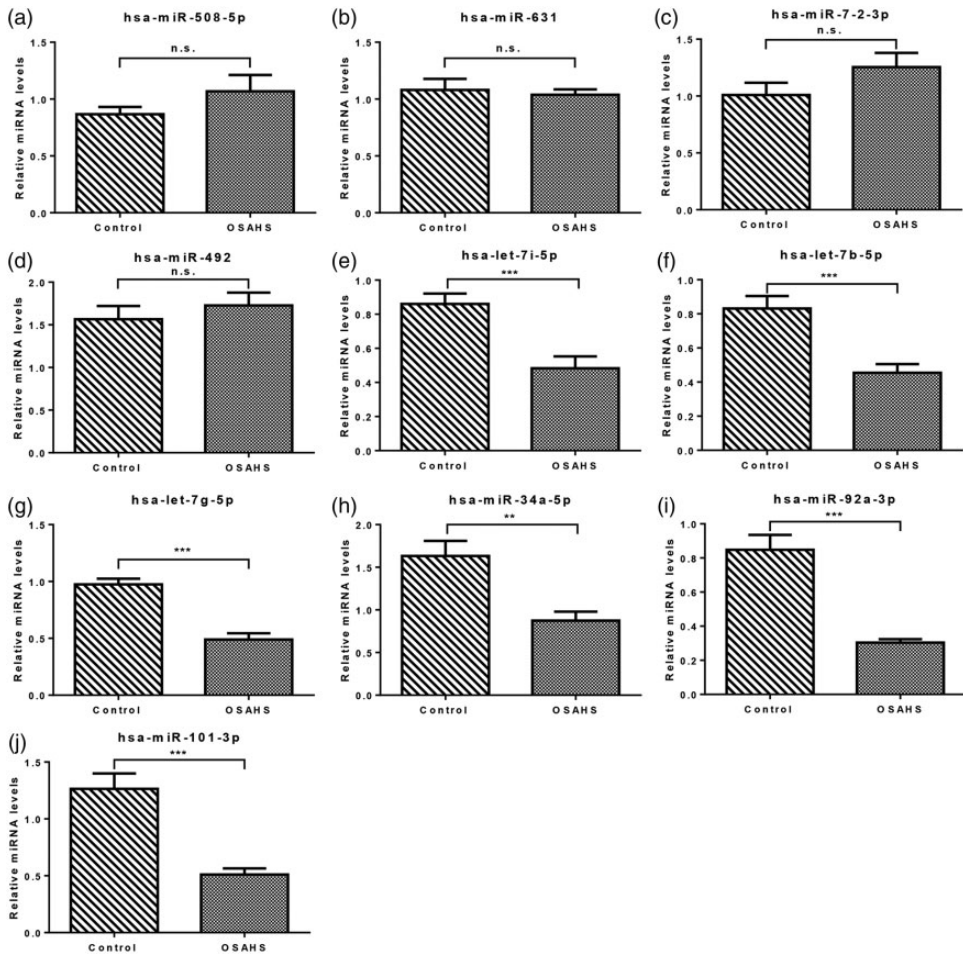


**Figure 2.** Validation of the differentially expressed miRNAs by qRT-PCR. Total RNA was isolated from 10 OSAHS patients and 10 controls. The expression levels of four upregulated miRNAs: (a) hsa-miR-508-5p, (b) hsa-miR-631, (c) hsa-miR-7-2-3p, and (d) hsa-miR-492, and six downregulated miRNAs: (e) hsa-let-7i-5p, (f) hsa-let-7b-5p, (g) hsa-let-7g-5p, (h) hsa-miR-34a-5p, (i) hsa-miR-92a-3p, and (j) hsa-miR-101-3p were measured by qRT-PCR to validate the array results. Bars represent the mean  $\pm$  SEM of each group; means of the two groups were compared by using a *t*-test: \*\**p* < 0.01, \*\*\**p* < 0.001, n.s. not significant. qRT-PCR, real-time quantitative PCR; OSAHS, obstructive sleep apnea-hypopnea syndrome; Ctrl, controls (patients with chronic tonsillitis but no OSAHS).

androgenic pathway and in mediating the transcriptional misregulation in cancers.

### Discussion

OSAHS is a common disorder characterized by recurrent UA collapse during sleep and it is a major public health concern.

The reduced or completely ceased airflow leads to arousals, sleep fragmentation, and oxyhemoglobin desaturation. The repetitive episodes of hypoxia and reoxygenation may result in systemic disorders, including metabolic disturbances, systemic inflammation, and cardiovascular diseases. In this study, we recruited 22 patients with severe OSAHS

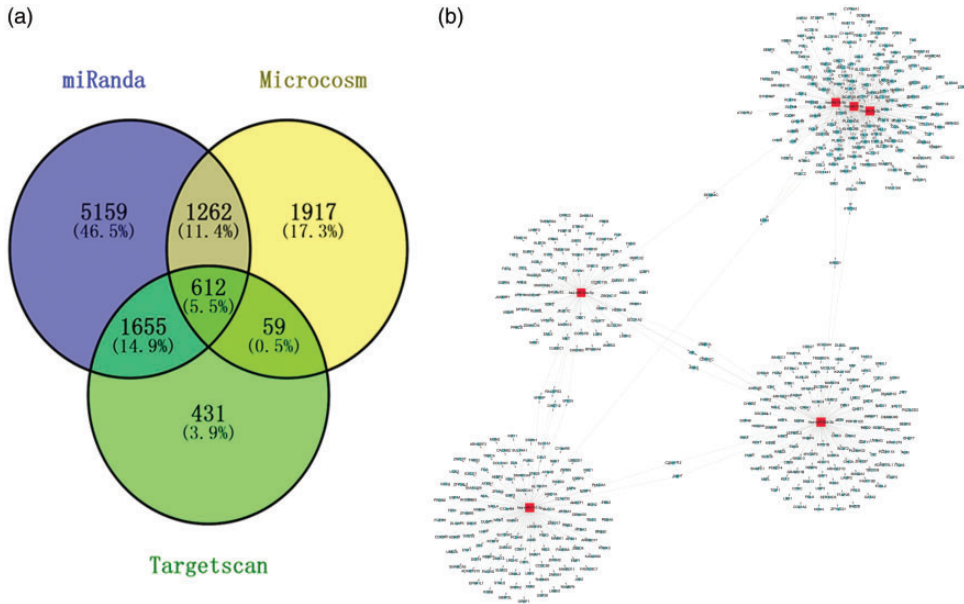


**Figure 3.** Prediction of miRNA targets and miRNA-gene regulatory network. The candidate target genes of the six downregulated miRNAs were predicted using miRanda, Microcosm, and Targetscan. (a) Venn diagram of predicted targets, showing that 8688, 3850, and 2757 targets were predicted by miRanda, Microcosm, and Targetscan, respectively, and 612 candidate genes were predicted by all three algorithms. (b) A miRNA-mRNA regulatory network based on the interactions between the six miRNAs and their potential targets. Red squares represent miRNAs, blue circular nodes represent candidate genes, and arrows from miRNAs to genes represent potential regulatory pairs.

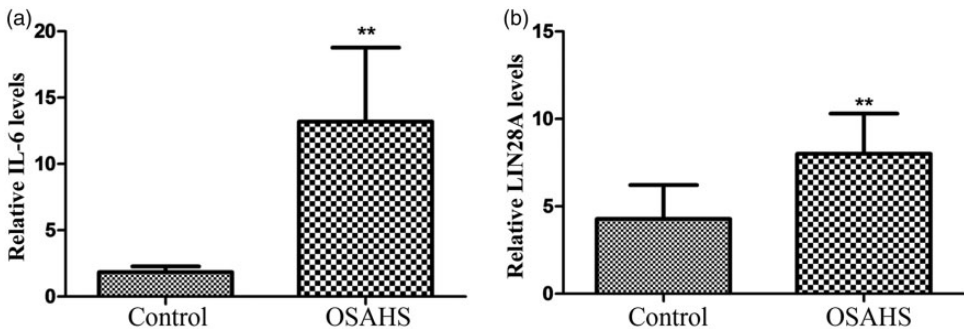


**Figure 4.** Expression of IL-6 and Lin28A mRNA was upregulated in OSAHS. Total RNA was isolated and mRNA expression levels of (a) IL-6 and (b) Lin28A were measured by qRT-PCR in 12 patients with OSAHS and 7 controls. The bars represent the mean  $\pm$  SEM of each group; means of the two groups were compared with the Mann-Whitney test:  $**p < 0.01$ . qRT-PCR, real-time quantitative PCR; OSAHS, obstructive sleep apnea-hypopnea syndrome; Ctrl, controls (patients with chronic tonsillitis but no OSAHS).





(AHI >30) and 17 patients with chronic tonsillitis without OSAHS as the control group (AHI <5). The OSAHS group had decreased minimum oxygen saturation and average oxygen saturation compared with the control group, suggesting an hypoxic status of these patients. In addition, the OSAHS group had significantly higher body mass index and triglyceride levels, suggesting that the OSAHS patients had profound metabolic abnormalities. These results are consistent with the reported spectrum of symptoms and comorbidities of OSAHS patients.<sup>1</sup>

A variety of contributing factors have been identified in the pathogenesis of OSAHS, including obesity, anatomical abnormalities, pharyngeal muscular dysfunction, ROS production, and systemic and local inflammation. Despite the rapidly growing list of factors, the exact etiopathogenesis of OSAHS remains largely unknown. Therefore, discovery of novel mechanism(s) for OSAHS development is beneficial in fully understanding the disease and developing preventive and therapeutic approaches. MiRNAs are key regulators of diverse biological processes, including development, differentiation, cell apoptosis, and proliferation. Recent studies have revealed that some miRNAs are associated with OSAHS-related morbidities. MiR-130a was involved in the progression of OSAHS-associated pulmonary hypertension by downregulating the *GAX* gene.<sup>22</sup> However, the involvement of miRNAs in the pathogenesis of OSAHS itself has not been reported.

Upper airway muscular dysfunction represents one of the most important pathophysiological factors of OSAHS and is the main cause of the UA collapse. The UA muscles of OSAHS patients are often exposed to hypoxia, mechanical stimulation, and inflammation. Altered miRNA profiles have been reported in cells or tissues exposed to these stimulating factors,

and the altered miRNA expression in turn may affect these processes. Hua et al.<sup>29</sup> reported that mechanical stretch regulates miRNA expression profile via nuclear factor- $\kappa$ B activation in C2C12 myoblasts. Mohamed et al.<sup>30</sup> showed that mechanical stretch selectively induced the transcription of miR-26a and led to human airway smooth muscle hypertrophy in severe asthma by suppressing glycogen synthase kinase-3 $\beta$  (GSK-3 $\beta$ ). Although it is possible that the miRNA profile in the UA muscles of OSAHS patients is altered, the miRNA expression profile has not previously been reported. In this study, we profiled miRNA expression in the UA skeletal muscles of four OSAHS patients and four controls by using a miRNA array assay. According to the criteria of fold change  $\geq 2.0$  and  $p < 0.05$ , 370 miRNAs were shown to be differentially expressed (181 upregulated and 189 downregulated) between OSAHS patients and controls. Therefore, the present study is the first, to the best of our knowledge, to reveal a global perturbation in the miRNA expression pattern in the UA muscle tissues of OSAHS patients.

We reviewed the literature on the differentially expressed miRNAs and found reports of several miRNAs that may be associated with the pathogenesis of OSAHS, in fat deposition, muscle tension reduction, inflammation edema, and other aspects. Considering the cost of analyzing more miRNAs, we selected four upregulated and six downregulated miRNAs from above to verify. The four upregulated miRNAs (hsa-miR-508-5p, hsa-miR-631, hsa-miR-7-2-3p, and hsa-miR-492) were validated by qRT-PCR in a cohort of 10 OSAHS patients and 10 controls. However, the levels of these four miRNAs were not significantly different between the OSAHS group and the control group (all  $p > 0.05$ ). qRT-PCR is a commonly used validation tool for confirming gene

expression results obtained from microarray analysis; however, microarray and qPCR data are often not in agreement. Any error in RNA extraction, labeling, hybridization, or signal reading might lead to false-positive results. In addition, the similarity in the sequence of miRNAs in the same family might account for false-positive results. For example, miR-508 belongs to the miR-506 family of miRNAs, which also includes miR-509 and miR-514.<sup>31,32</sup> The array might mistakenly read the signal of other family members as miR-508 because of cross-hybridization of these closely related miRNAs with similar sequences. In contrast to the upregulated miRNAs, the six selected downregulated miRNAs (hsa-let-7i-5p, hsa-let-7b-5p, hsa-let-7g-5p, hsa-miR-34a-5p, hsa-miR-92a-3p, and hsa-miR-101-3p) were all validated by qRT-PCR in the same cohort of samples (all  $p < 0.05$ ) (Figure 2a-j, Table 2). To date, 10 members of the let-7 family have been identified in humans, including let-7a, let-7b, let-7c, let-7d, let-7e, let-7f, let-7g, let-7i, miR-98, and miR-202.<sup>33</sup> The let-7 family of miRNAs is reported to be widely involved in inflammation,<sup>34</sup> cell metabolism,<sup>35</sup> response to hypoxia,<sup>36</sup> and muscle structure.<sup>37</sup> miR-34a, miR-92a and miR-101 were also associated with inflammation,<sup>38-41</sup> hypoxia,<sup>42-44</sup> and muscle structure,<sup>45-47</sup> all aspects related to OSAHS. Therefore, we selected these miRNAs for validation by qRT-PCR and further bioinformatics analyses. Our results suggested that the array data included a lot of false-positive results; therefore, before initiating further investigations of miRNAs, they must be validated by qRT-PCR.

Systemic and local inflammation is involved in OSAHS and its comorbidities. Intermittent hypoxia caused by OSAHS has been associated with systematic inflammation, with production of inflammatory cytokines such as IL-6 and TNF- $\alpha$ . However, it

is still unclear whether systemic inflammation is a cause or a result of OSAHS. Moreover, repeated snoring, hypoxia, and other factors may lead to mechanical trauma and local inflammation of UA muscle tissues. Local inflammation in turn leads to alterations in muscle fiber structure, which forms the histological basis for the dysfunction of UA or lower pharynx neuromuscular tissues during sleep. In this study, we found that three let-7 family members, hsa-let-7b-5p, hsa-let-7g-5p, and hsa-let-7i-5p, were downregulated in UA muscle tissues of OSAHS. IL-6 is a proinflammatory factor and has been reported to be a target of these three miRNAs. Our qRT-PCR data showed that IL-6 was significantly upregulated in OSAHS patients, suggesting that the downregulated let-7 family members might contribute to local inflammation in OSAHS by upregulating IL-6.

Lin28A and Lin28B are selective suppressors of let-7 miRNA expression and function as oncogenes in a variety of human cancers. They specifically bind to the let-7 precursors and recruit ZCCHC11/TUT4 uridylyltransferase, which introduces terminal uridylation. Uridylated prelet-7s fail to be processed by Dicer and undergo degradation<sup>48,49</sup>. Moreover, Lin28A has been predicted to be a target of the three let-7 family miRNAs mentioned above. In this study, Lin28A was also upregulated in the UA muscles tissues of OSAHS patients (Figure 4), suggesting a potential negative regulatory loop accounting for the downregulation of the three let-7 miRNAs. Further studies, such as luciferase reporter assays, are necessary to confirm this hypothesis.

A set of target genes regulated by an individual miRNA generally constitutes a biological network of functionally associated molecules in human cells. Therefore, it is important to gain deeper insights into the biological implications of the target networks of these six miRNAs. In our

experiment, 612 targets were predicted and could serve as the basis for future experiments. The GO and KEGG enrichment analyses revealed the profoundly perturbed signaling pathways and cellular functions in the UA muscles of OSAHS patients caused by altered miRNA expression.

The limitations of this study need to be addressed. The control group was a cohort of patients with chronic tonsillitis, a disease that represents a chronic inflammation state, which might lead to perturbation of miRNA profile and subsequent downstream gene changes, therefore compromising our conclusion. We failed to validate the four upregulated genes by qRT-PCR, suggesting the existence of false-positive results in the array data. Study of any candidate miRNA in the array needs to first validate its differential expression. Furthermore, the target genes of the six downregulated miRNAs were predicted by bioinformatics algorithms. Although we included only targets predicted by all three algorithms in our analysis, the possibility of false prediction remains. Therefore, the functional and pathways analyses based on these predicted targets may introduce bias. In future studies, we need to examine the transcriptional profile together with the miRNA profile and repeat the bioinformatics analyses. This study analyzed only 6 of 380 potentially dysregulated miRNAs; therefore, more miRNAs must be investigated to reveal the complete picture of dysregulated signaling pathways and cellular functions in UA muscular tissue of OSAHS patients. In addition, functional studies of candidate miRNAs in OSAHS cell lines or animal models are warranted.

In summary, we identified a perturbed miRNA profile in the UA muscles of OSAHS patients. These dysregulated miRNAs potentially led to profound alterations in signaling pathways and cellular functions, which might have contributed to the pathogenesis of OSAHS. Some of

these miRNAs were associated with local inflammation by upregulating inflammatory factors, such as IL-6. This study is the first to reveal an altered miRNA profile in the UA muscular tissue of OSAHS patients and therefore provides a theoretical basis for developing novel miRNA-based interventions of OSAHS.

### Declaration of conflicting interest

The authors declare that there is no conflict of interest.

### Funding

This work was supported by the funding from Natural Science Foundation of Shaanxi Province (No. 2016SF-125).

### ORCID iD

Min Xu  <https://orcid.org/0000-0001-7544-7913>

### References

1. White DP. Advanced concepts in the pathophysiology of obstructive sleep apnea. *Adv Otorhinolaryngol* 2017; 80: 7–16.
2. Punjabi NM. The epidemiology of adult obstructive sleep apnea. *Proc Am Thorac Soc* 2008; 5: 136–143.
3. Ip MS, Lam B, Ng MM, et al. Obstructive sleep apnea is independently associated with insulin resistance. *Am J Respir Crit Care Med* 2002; 165: 670–676.
4. Reichmuth KJ, Austin D, Skatrud JB, et al. Association of sleep apnea and type II diabetes: a population-based study. *Am J Respir Crit Care Med* 2005; 172: 1590–1595.
5. Tamaki S, Yamauchi M, Fukuoka A, et al. Production of inflammatory mediators by monocytes in patients with obstructive sleep apnea syndrome. *Intern Med* 2009; 48: 1255–1262.
6. Nieto FJ, Young TB, Lind BK, et al. Association of sleep-disordered breathing, sleep apnea, and hypertension in a large community-based study. Sleep Heart Health Study. *JAMA* 2000; 283: 1829–1836.

7. Dempsey JA, Veasey SC, Morgan BJ, et al. Pathophysiology of sleep apnea. *Physiol Rev* 2010; 90: 47–112.
8. Parati G, Lombardi C and Narkiewicz K. Sleep apnea: epidemiology, pathophysiology, and relation to cardiovascular risk. *Am J Physiol Regul Integr Comp Physiol* 2007; 293: R1671–R1683.
9. Ryan S, Taylor CT and McNicholas WT. Selective activation of inflammatory pathways by intermittent hypoxia in obstructive sleep apnea syndrome. *Circulation* 2005; 112: 2660–2667.
10. Gozal D, Capdevila OS and Kheirandish-Gozal L. Metabolic alterations and systemic inflammation in obstructive sleep apnea among nonobese and obese prepubertal children. *Am J Respir Crit Care Med* 2008; 177: 1142–1149.
11. Unnikrishnan D, Jun J and Polotsky V. Inflammation in sleep apnea: an update. *Rev Endocr Metab Disord* 2015; 16: 25–34.
12. Yokoe T, Minoguchi K, Matsuo H, et al. Elevated levels of C-reactive protein and interleukin-6 in patients with obstructive sleep apnea syndrome are decreased by nasal continuous positive airway pressure. *Circulation* 2003; 107: 1129–1134.
13. Reyad E, Abdelaty NM, Prince ME, et al. Plasma levels of TNF in obstructive sleep apnea syndrome (OSA) before and after surgical intervention. *Egypt J Chest Dis Tuberc* 2012; 61: 179–185.
14. Boyd JH, Petrof BJ, Hamid Q, et al. Upper airway muscle inflammation and denervation changes in obstructive sleep apnea. *Am J Respir Crit Care Med* 2004; 170: 541–546.
15. Fritscher LG, Mottin CC, Canani S, et al. Obesity and obstructive sleep apnea-hypopnea syndrome: the impact of bariatric surgery. *Obes Surg* 2007; 17: 95–99.
16. Lavie L and Lavie P. Molecular mechanisms of cardiovascular disease in OSAHS: the oxidative stress link. *Eur Respir J* 2009; 33: 1467–1484.
17. Dudley KA and Patel SR. Disparities and genetic risk factors in obstructive sleep apnea. *Sleep Med* 2016; 18: 96–102.
18. Yalcinkaya M, Erbek SS, Babakurban ST, et al. Lack of association of matrix metalloproteinase-9 promoter gene polymorphism in obstructive sleep apnea syndrome. *J Craniomaxillofac Surg* 2015; 43: 1099–1103.
19. Ding Y, Ma Q, Liu F, et al. The potential use of salivary miRNAs as promising biomarkers for detection of cancer: a meta-analysis. *PLoS One* 2016; 11: e0166303.
20. Hao M, Zang M, Zhao L, et al. Serum high expression of miR-214 and miR-135b as novel predictor for myeloma bone disease development and prognosis. *Oncotarget* 2016; 7: 19589–19600.
21. Gharib SA, Khalyfa A, Abdelkarim A, et al. Intermittent hypoxia activates temporally coordinated transcriptional programs in visceral adipose tissue. *J Mol Med (Berl)* 2012; 90: 435–445.
22. An Z, Wang D, Yang G, et al. Role of microRNA-130a in the pathogenesis of obstructive sleep apnea hypopnea syndrome-associated pulmonary hypertension by targeting the GAX gene. *Medicine (Baltimore)* 2017; 96: e6746.
23. Zhang B, Qiangba Y, Shang P, et al. A comprehensive microRNA expression profile related to hypoxia adaptation in the Tibetan pig. *PLoS One* 2015; 10: e0143260.
24. Zheng J, Zhang K, Wang Y, et al. Identification of a microRNA signature in endothelial cells with mechanical stretch stimulation. *Mol Med Rep* 2015; 12: 3525–3530.
25. Ortega FJ, Moreno M, Mercader JM, et al. Inflammation triggers specific microRNA profiles in human adipocytes and macrophages and in their supernatants. *Clin Epigenetics* 2015; 7: 49.
26. Starr TK, Scott PM, Marsh BM, et al. A Sleeping Beauty transposon-mediated screen identifies murine susceptibility genes for adenomatous polyposis coli (Apc)-dependent intestinal tumorigenesis. *Proc Natl Acad Sci U S A* 2011; 108: 5765–5770.
27. Huat TJ, Khan AA, Abdullah JM, et al. MicroRNA expression profile of neural progenitor-like cells derived from rat bone

- marrow mesenchymal stem cells under the influence of IGF-1, bFGF and EGF. *Int J Mol Sci* 2015; 16: 9693–9718.
28. Liu X, Wu Y, Huang Q, et al. Grouping pentylenetetrazol-induced epileptic rats according to memory impairment and microRNA expression profiles in the hippocampus. *PLoS One* 2015; 10: e0126123.
  29. Hua W, Zhang M, Wang Y, et al. Mechanical stretch regulates microRNA expression profile via NF-kappaB activation in C2C12 myoblasts. *Mol Med Rep* 2016; 14: 5084–5092.
  30. Mohamed JS, Lopez MA and Boriek AM. Mechanical stretch up-regulates microRNA-26a and induces human airway smooth muscle hypertrophy by suppressing glycogen synthase kinase-3beta. *J Biol Chem* 2010; 285: 29336–29347.
  31. Bagnoli M, De Cecco L, Granata A, et al. Identification of a chrXq27.3 microRNA cluster associated with early relapse in advanced stage ovarian cancer patients. *Oncotarget* 2011; 2: 1265–1278.
  32. Zhai Q, Zhou L, Zhao C, et al. Identification of miR-508-3p and miR-509-3p that are associated with cell invasion and migration and involved in the apoptosis of renal cell carcinoma. *Biochem Biophys Res Commun* 2012; 419: 621–626.
  33. Thammaiah CK and Jayaram S. Role of let-7 family microRNA in breast cancer. *Noncoding RNA Res* 2016; 1: 77–82.
  34. Polikepahad S, Knight JM, Naghavi AO, et al. Proinflammatory role for let-7 microRNAs in experimental asthma. *J Biol Chem* 2010; 285: 30139–30149.
  35. Kuppusamy KT, Jones DC, Sperber H, et al. Let-7 family of microRNA is required for maturation and adult-like metabolism in stem cell-derived cardiomyocytes. *Proc Natl Acad Sci U S A* 2015; 112: E2785–E2794.
  36. Joshi S, Wei J and Bishopric NH. A cardiac myocyte-restricted Lin28/let-7 regulatory axis promotes hypoxia-mediated apoptosis by inducing the AKT signaling suppressor PIK3IP1. *Biochim Biophys Acta* 2015; 1862: 240–251.
  37. Shenoy A and Belloch RH. Regulation of microRNA function in somatic stem cell proliferation and differentiation. *Nat Rev Mol Cell Biol* 2014; 15: 565–576.
  38. Bu P, Wang L, Chen KY, et al. A miR-34a-numb feedforward loop triggered by inflammation regulates asymmetric stem cell division in intestine and colon cancer. *Cell Stem Cell* 2016; 18: 189–202.
  39. Jiang P, Liu R, Zheng Y, et al. MiR-34a inhibits lipopolysaccharide-induced inflammatory response through targeting Notch1 in murine macrophages. *Exp Cell Res* 2012; 318: 1175–1184.
  40. Lai L, Song Y, Liu Y, et al. MicroRNA-92a negatively regulates Toll-like receptor (TLR)-triggered inflammatory response in macrophages by targeting MKK4 kinase. *J Biol Chem* 2013; 288: 7956–7967.
  41. Zheng Y, Wang Z, Tu Y, et al. miR-101a and miR-30b contribute to inflammatory cytokine-mediated beta-cell dysfunction. *Lab Invest* 2015; 95: 1387–1397.
  42. Du R, Sun W, Xia L, et al. Hypoxia-induced down-regulation of microRNA-34a promotes EMT by targeting the Notch signaling pathway in tubular epithelial cells. *PLoS One* 2012; 7: e30771.
  43. Zhang B, Zhou M, Li C, et al. MicroRNA-92a inhibition attenuates hypoxia/reoxygenation-induced myocardocyte apoptosis by targeting Smad7. *PLoS One* 2014; 9: e100298.
  44. Kim JH, Lee KS, Lee DK, et al. Hypoxia-responsive microRNA-101 promotes angiogenesis via heme oxygenase-1/vascular endothelial growth factor axis by targeting cullin 3. *Antioxid Redox Signal* 2014; 21: 2469–2482.
  45. Badi I, Burba I, Ruggeri C, et al. MicroRNA-34a induces vascular smooth muscle cells senescence by SIRT1 downregulation and promotes the expression of age-associated pro-inflammatory secretory factors. *J Gerontol A Biol Sci Med Sci* 2015; 70: 1304–1311.
  46. Zhang L, Zhou M, Wang Y, et al. miR-92a inhibits vascular smooth muscle cell

- apoptosis: role of the MKK4-JNK pathway. *Apoptosis* 2014; 19: 975–983.
47. Beauchemin M, Smith A and Yin VP. Dynamic microRNA-101a and Fosab expression controls zebrafish heart regeneration. *Development* 2015; 142: 4026–4037.
48. Piskounova E, Polytarchou C, Thornton JE, et al. Lin28A and Lin28B inhibit let-7 microRNA biogenesis by distinct mechanisms. *Cell* 2011; 147: 1066–1079.
49. Balzeau J, Menezes MR, Cao S, et al. The LIN28/let-7 pathway in cancer. *Front Genet* 2017; 8: 31.